blood®
Regular Article

TRANSPLANTATION

BET-bromodomain and EZH2 inhibitor–treated chronic GVHD mice have blunted germinal centers with distinct transcriptomes

Michael C. Zaiken,[1] Ryan Flynn,[1] Katelyn G. Paz,[1] Stephanie Y. Rhee,[1] Sujeong Jin,[1] Fathima A. Mohamed,[1] Asim Saha,[1] Govindarajan Thangavelu,[1] Paul M. C. Park,[2] Matthew L. Hemming,[2] Peter T. Sage,[3,4] Arlene H. Sharpe,[3,4] Michel DuPage,[5] Jeffrey A. Bluestone,[6] Angela Panoskaltsis-Mortari,[1] Corey S. Cutler,[7] John Koreth,[7] Joseph H. Antin,[7] Robert J. Soiffer,[8] Jerome Ritz,[7] Leo Luznik,[9] Ivan Maillard,[10] Geoffrey R. Hill,[11,12] Kelli P. A. MacDonald,[13] David H. Munn,[14] Jonathan S. Serody,[15] William J. Murphy,[16] Leslie S. Kean,[2,17] Yi Zhang,[18] James E. Bradner,[19] Jun Qi,[2,20] and Bruce R. Blazar[1]

[1]Division of Blood & Marrow Transplant & Cellular Therapy, Department of Pediatrics, Masonic Cancer Center, University of Minnesota, Minneapolis, MN; [2]Department of Cancer Biology, Dana-Farber Cancer Institute, Boston, MA; [3]Department of Immunology, Blavatnik Institute, Harvard Medical School, Boston, MA; [4]Evergrande Center for Immunologic Diseases, Harvard Medical School–Brigham and Women's Hospital, Boston, MA; [5]Division of Immunology and Pathogenesis, Department of Molecular and Cell Biology, University of California Berkeley, Berkeley, CA; [6]University of California San Francisco, San Francisco, CA; [7]Division of Hematologic Malignancies, [8]Department of Medical Oncology, Dana-Farber Cancer Institute, Harvard Medical School, Boston, MA; [9]Department of Oncology, Sidney Kimmel Cancer Center, Baltimore, MD; [10]Division of Hematology-Oncology, Department of Medicine, University of Pennsylvania, Philadelphia, PA; [11]Clinical Research Division, Fred Hutchinson Cancer Research Center, Seattle, WA; [12]Division of Medical Oncology, University of Washington, Seattle, WA; [13]Department of Immunology, Queensland Institute of Medical Research (QIMR), University of Queensland, Brisbane, QLD, Australia; [14]Georgia Cancer Center, Augusta University, Augusta, GA; [15]Lineberger Comprehensive Cancer Center, University of North Carolina, Chapel Hill, NC; [16]Department of Dermatology, School of Medicine, University of California, Davis, Sacramento, CA; [17]Boston Children's Hospital, Dana-Farber Cancer Institute, Boston, MA; [18]Fels Institute for Cancer Research and Molecular Biology, Department of Microbiology and Immunology, Temple University, Philadelphia, PA; [19]Department of Medical Oncology, Dana-Farber Cancer Institute, Boston, MA; and [20]Department of Medicine, Harvard Medical School, Boston, MA

KEY POINTS

- **Novel EZH2 inhibitor JQ5 and BET-bromodomain inhibitor JQ1 reduce pulmonary dysfunction and blunt GC response in murine cGVHD.**
- **Despite similar physiological impacts, JQ1 and JQ5 induce distinct transcriptional changes that independently disrupt the GC.**

Despite advances in the field, chronic graft-versus-host-disease (cGVHD) remains a leading cause of morbidity and mortality following allogenic hematopoietic stem cell transplant. Because treatment options remain limited, we tested efficacy of anticancer, chromatin-modifying enzyme inhibitors in a clinically relevant murine model of cGVHD with bronchiolitis obliterans (BO). We observed that the novel enhancer of zeste homolog 2 (EZH2) inhibitor JQ5 and the BET-bromodomain inhibitor JQ1 each improved pulmonary function; impaired the germinal center (GC) reaction, a prerequisite in cGVHD/BO pathogenesis; and JQ5 reduced EZH2-mediated H3K27me3 in donor T cells. Using conditional EZH2 knockout donor cells, we demonstrated that EZH2 is obligatory for the initiation of cGVHD/BO. In a sclerodermatous cGVHD model, JQ5 reduced the severity of cutaneous lesions. To determine how the 2 drugs could lead to the same physiological improvements while targeting unique epigenetic processes, we analyzed the transcriptomes of splenic GCB cells (GCBs) from transplanted mice treated with either drug. Multiple inflammatory and signaling pathways enriched in cGVHD/BO GCBs were reduced by each drug. GCBs from JQ5- but not JQ1-treated mice were enriched for proproliferative pathways also seen in GCBs from bone marrow-only transplanted mice, likely reflecting their underlying biology in the unperturbed state. In conjunction with in vivo data, these insights led us to conclude that epigenetic targeting of the GC is a viable clinical approach for the treatment of cGVHD, and that the EZH2 inhibitor JQ5 and the BET-bromodomain inhibitor JQ1 demonstrated clinical potential for EZH2i and BETi in patients with cGVHD/BO.

Introduction

Chronic graft-versus-host disease (cGVHD) is a life-threatening, multiorgan, autoimmune-like condition that arises late following allogeneic hematopoietic stem cell transplantation (alloHSCT). Despite recent advances, cGVHD remains the leading cause of morbidity and nonrelapse associated mortality following alloHSCT, arising in 30% to 70% of patients.[1-6] Treatment options remain limited. First-line treatment involves corticosteroids resulting in a 50% to 60% response rate, more global immunosuppression, and potential serious side effects.[7] There has been increasing emphasis on more immunomodulatory and less immunosuppressive pharmacologic agents. Ibrutinib, a Bruton tyrosine kinase and interleukin 2 (IL-2)-inducible kinase (ITK) inhibitor, was the first approved therapy for patients with steroid-refractory cGVHD failing systemic therapies.[5,6] Belumosudil (KD025; Rezurock), a ρ-associated coiled-coil kinase 2

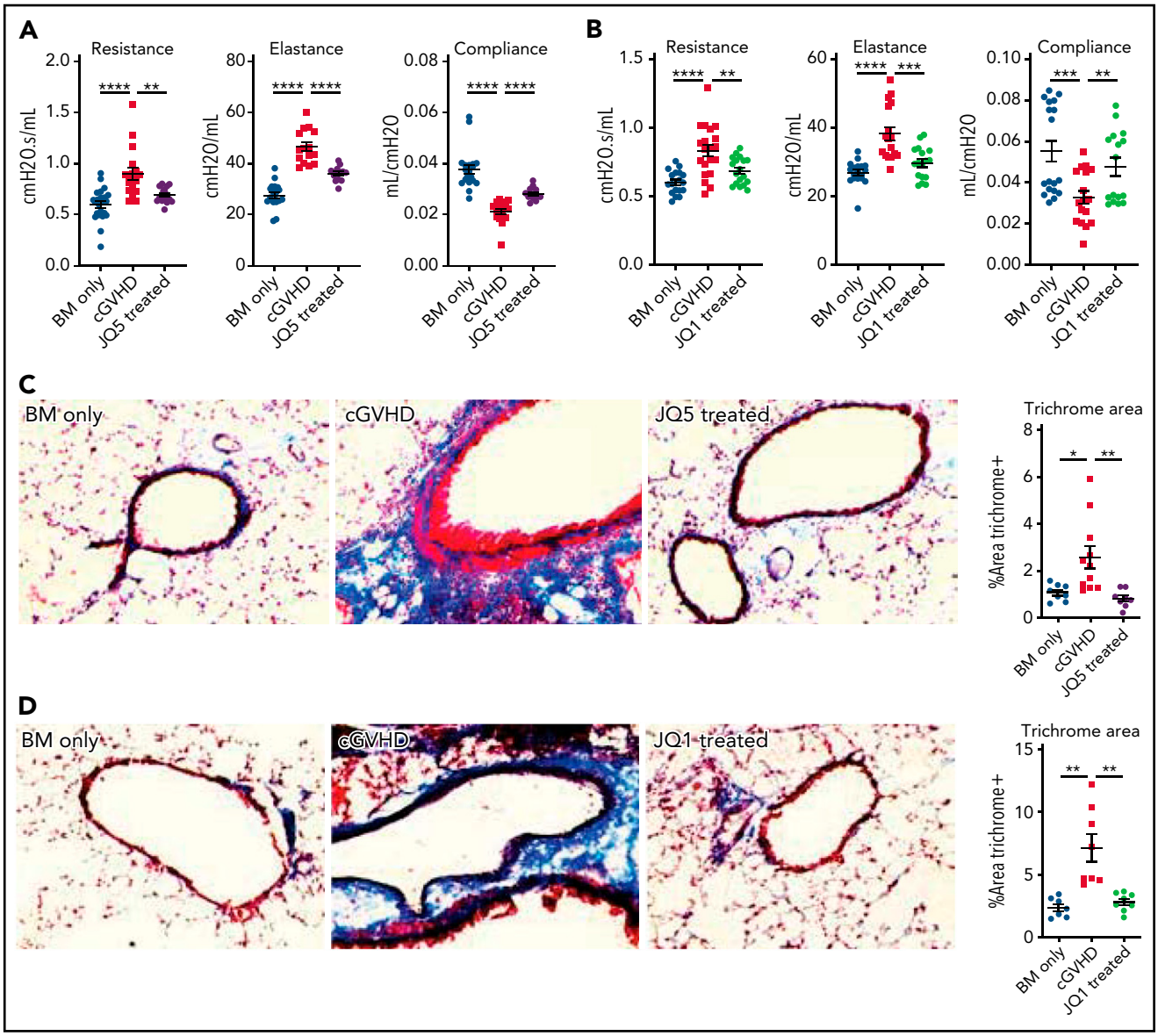

Figure 1. JQ5 and JQ1 treat murine cGVHD/BO. Results are from BO cGVHD transplants. B10.BR mice were conditioned with 120 mg/kg Cytoxan (cyclophosphamide) (days −3, −2) and 7.6 Gy total body irradiation (TBI) (day −1). On day 0, recipients received 10×10^6 purified BM cells ± 73.5×10^3 B6 purified T cells from C57BL/6. Groups included a BM-only negative control, a WT BM and T-cell–positive control, and mice that were given each treatment either JQ5 (75 mg/kg 3×/wk) or JQ1 (50 mg/kg 3× per week) from day 28 to day 49 posttransplant. Results shown are pooled from 3 transplant replicates. Results of pulmonary function tests taken on day 49 posttransplant include measures of resistance, elastance, and compliance. Significant improvement in pulmonary function across multiple parameters was observed with both JQ5 (A; n = 22/BM-only, n = 17/cGVHD, n = 15/JQ5) and JQ1 (B; n = 18/BM-only, n = 20/cGVHD, n = 18/JQ1) treatment. Representative images of cryopreserved lung sections from mice 49 days posttransplant. (C-D) Sections were stained with Masson trichrome and analyzed for collagen deposition. Quantification of the trichrome positive area is in the furthest right panel. This deposition is significantly reduced in both the JQ5-treated mice (C; n = 8/BM-only, n = 11/cGVHD, n = 8/JQ5) and the JQ1 treated mice (D; n = 7/BM-only, n = 8/cGVHD, n = 8/JQ1). (E-F) Sections were stained with anti IgG FITC and DAPI and show a reduction of IgG^+ tissue in both JQ5-treated mice (E; n = 5/BM-only, n = 5/cGVHD, n = 4/JQ5) and the JQ1-treated mice (F; n = 5/BM-only, n = 5/cGVHD, n = 4/JQ1). Quantification of $FITC^+$ area is shown in panels furthest to the right. All images are at ×200 magnification. Statistics shown are results of an unpaired *t* test with Bonferroni corrected *P* values when appropriate. $^*P < .05$, $^{**}P < .01$, $^{***}P < .001$, $^{****}P < .0001$.

inhibitor, was approved for patients with cGVHD failing 2 or more lines of systemic therapy.[8] In a randomized phase 3 trial, ruxolitinib (Jakafi), a JAK1/2 inhibitor, showed superiority for treating steroid-refractory or steroid-dependent patients with cGVHD failing <2 prior systemic therapies most recently received US Food and Drug Administration (FDA) approval.[9] Complete responses were infrequent and drug-associated side effects (eg, cytopenias and infections) were observed, demonstrating a clear medical need for additional therapies.

Of the cGVHD manifestations, sclerodermatous and pulmonary cGVHD remain treatment challenges.[10,11] Well-established preclinical murine scleroderma models have been used as a platform for testing new agents.[12,13] A murine multiorgan system cGVHD

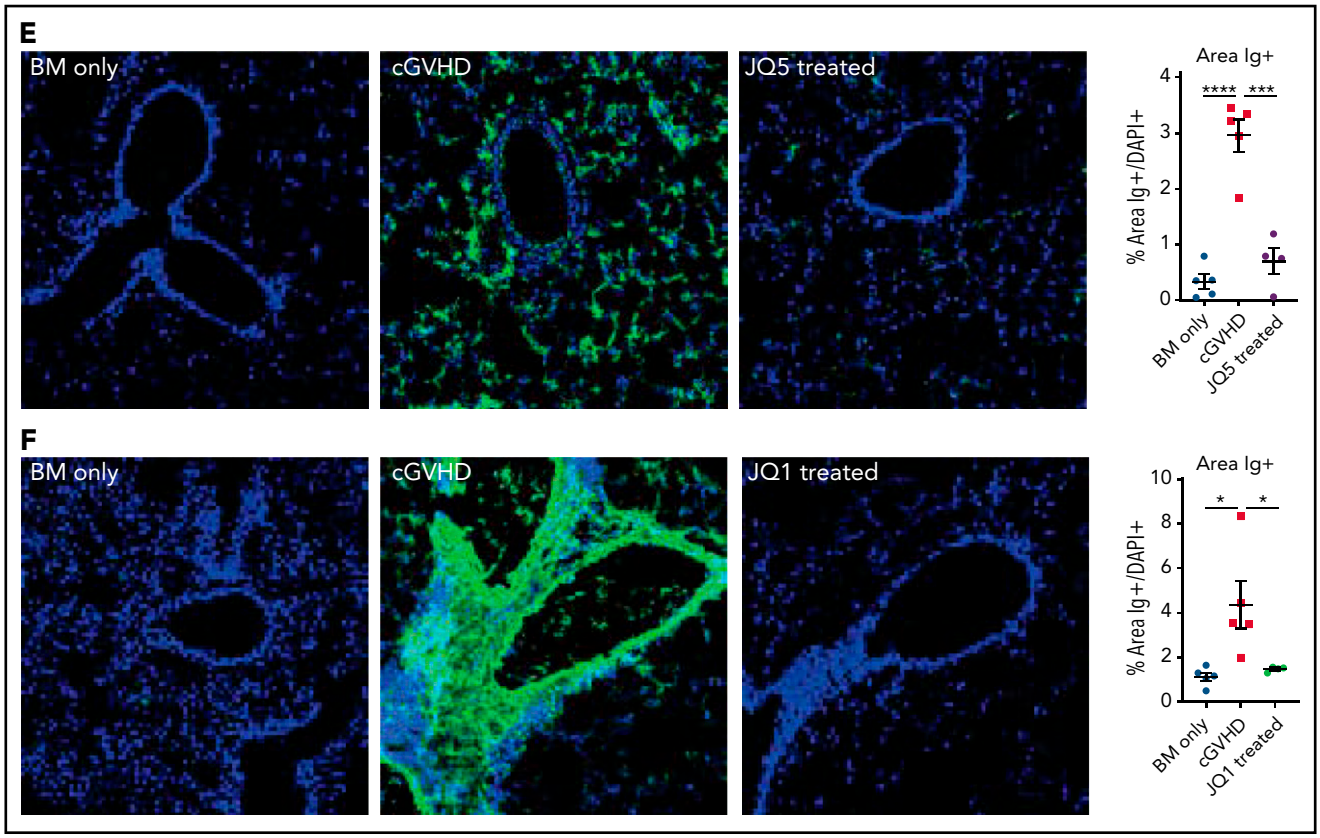

Figure 1. (continued)

model with bronchiolitis obliterans (BO) was developed that is germinal center (GC) formation dependent. The production and lung deposition of allo- and/or autoantibodies, monocyte and macrophage recruitment, and activation results in profibrogenic molecule release, fibroblast secretion of extracellular matrix including collagen, and fibrosis, suggesting that modulation or inhibition of the GC reaction may be a new therapeutic target.[14-16]

Enhancer of Zeste homolog 2 (EZH2), a histone-lysine *N*-methyltransferase and the catalytic component of the polycomb repressive complex 2 is a critical regulator in GC formation and proliferation/differentiation of antibody secreting B cells.[17,18] EZH2 catalyzes the trimethylation of lysine 27 on histone 3 (H3K27me3), impairing target gene transcription, and has a key role in establishing bivalent chromatin domains that regulate cell fate determination.[19-24] EZH2 overexpression is seen in a diffuse array of tumors, including B- and T-cell malignancies,[25] and is associated with a poor prognosis.[26,27] Of available EZH2 inhibitors, we tested a readily translatable, high potency, and bioavailable compound, JQEZ5 (JQ5), for effects in sclerodermatous and cGVHD/BO models.[28]

Other GC targeting were directed to bromodomain and extraterminal (BET) enzymes. Bromodomains (BRDs) recognize histone acetylated lysine motifs and initiate transcriptional activation to drive gene expression. Small molecule inhibitors competitively bind BRD, preventing histone acetylated lysine engagement, decreasing expression of genes involved in cell proliferation, differentiation, and cytokine/chemokine production.[29] For example, in vitro the BET inhibitor JQ1 hinders T-cell IL-21 expression required for T-follicular helper cell (TFH) function.[30] In vivo JQ1 impaired GC B-cell (GCB) formation via BCL6 repression in 4-hydroxy-3-nitrophenyl-chicken γ globulin-immunized mice.[31] In culture and murine systemic lupus erythematosus models, cytokines, B-cell activating factor, and IL-17, implicated in cGVHD pathology, were suppressed. In a murine acute GVHD (aGVHD) model, the selective pan-BET inhibitor, I-BET151, reduced inflammatory cytokines, improving survival and pathology.[32] These properties pointed to JQ1 therapeutic potential for sclerodermatous and pulmonary cGVHD.

Because both EZH2 and BRD4 are upregulated in GCBs, we hypothesized that JQ1 and JQ5 would effectively treat murine cGVHD/BO. In testing this, we investigated JQ5 and JQ1 as novel treatments for cGVHD, established EZH2 necessity in both the bone marrow (BM) and T-cell graft compartments for cGVHD/BO initiation, and identified that JQ5 has therapeutic potential in both BO and sclerodermatous cGVHD models, whereas JQ1 only mitigated disease in a cGVHD/BO model. By comparing GCB transcriptomes from mice with cGVHD/BO treated with each compound, we offer potential mechanistic explanations for these observations. Given the recent FDA approval of EZH2 inhibitors and more than a dozen BRD inhibitors in clinical trials, our study helps establish the preclinical rationale on both targets for cGVHD treatment.

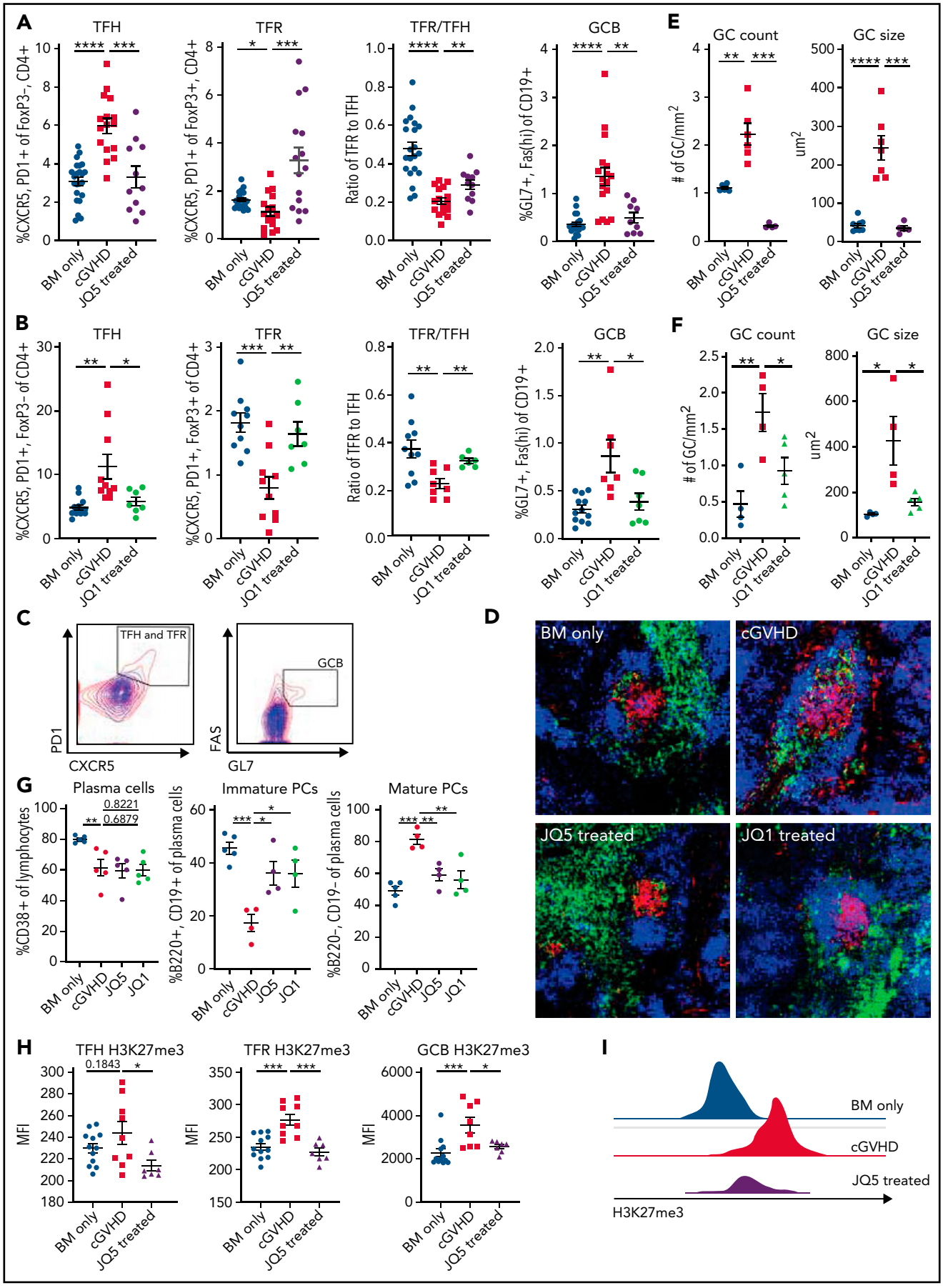

Figure 2.

Materials and methods

Mice

C57Bl/6 (B6) ($H2^b$) mice were purchased from the National Cancer Institute through Charles River Laboratories. B10.BR ($H2^k$), BALB/c ($H2^d$), and B10.D2 ($H2^d$) mice were purchased from The Jackson Laboratories. EZH2 fl/fl provided by M.D. and J.A.B. were bred to CD4-Cre and CD19-Cre mice at the University of Minnesota animal facility.[33,34] All mice were housed in a specific pathogen-free facility and used with University of Minnesota Institutional Animal Care and Use Committee approval.

Bone marrow transplant

In the cGVHD/BO model, B10.BR recipients were conditioned with 120 mg/kg Cytoxan (days −3, −2) and 7.6 Gy total body irradiation (TBI) (day −1). Donor (B6) BM was T-cell–depleted with anti-CD4/anti-CD8 monoclonal antibodies and rabbit complement. Splenic T cells were purified using anti-CD19 (13-0193-85eBio), anti-B220 (60019BT; Stemcell Technologies), anti-CD11b (60001BT; Stemcell Technologies), anti-CD11c (60002BT; Stemcell Technologies), anti-TCRγ/δ (553176 Becton Dickinson [BD]), anti-NK1.1 (13-5941-85; eBio), and anti-TER119 (13-5921-85 eBio) antibodies and magnetic beads (50001; Stemcell Technologies). Recipients received 10×10^6 purified BM cells ± 73.5×10^3 B6 purified T cells. Mice were monitored daily for survival, clinical and skin scores were done twice weekly, and weights recorded weekly.[14,16] In the sclerodermatous model, B10.D2 BM (10×10^6) and T cells (2.7×10^6; 2:1 CD4:CD8 ratio) were given to BALB/c recipients after 7.0 Gy TBI (day −1).[35] Mice were monitored daily and assessed for clinical score and skin score as described.[36]

JQ1 and JQ5 preparation and administration

JQ5 and JQ1 were provided by J.E.B. and J.Q.[28,37] Both compounds were characterized using nuclear magnetic resonance, high-resolution mass spectrometry, and high-performance liquid chromatography to confirm the identity and purity. JQ5 was synthesized and purified by flash chromatography and prep-high-performance liquid chromatography.[37] JQ1 was synthesized to produce racemic JQ1, as published.[28] cGVHD mice were injected intraperitoneally with JQ5 (75 mg/kg) or JQ1 (50 mg/kg) in 10% 2-hydroxypropyl)-β-cyclodextrin or vehicle 3 times weekly from day 28 (cGVHD/BO onset) until day 49.

Pulmonary function tests

Mice were anesthetized and ventilated using the Flexivent system (Scireq). Pulmonary resistance, elastance, and compliance were measured using Flexivent Software v5.1.[14]

Frozen tissue preparation

At time of euthanization, lungs were intratracheally inflated with 75% Tissue-Tek optimal cutting temperature compound (catalog no. 4583). Tissue blocks were flash frozen and stored at −80°C.

Immunofluorescence

For immunofluorescence assays, 8-μm cryosections were cut and acetone fixed. For immunoglobulin (Ig) deposition experiments, lung sections were stained with goat anti-mouse FITC conjugated antibody (BD; 553585), and DAPI (4′,6-diamidino-2-phenylindole) containing mounting medium (H-2000-10; Vector Laboratories). For GC detection, spleen sections were stained with rhodamine-peanut agglutinin (RL-1072; Vector Laboratories), anti-CD4 FITC (11-0042-82; ThermoFisher) antibody and mounted in DAPI mounting medium (H-2000-10; Vector Laboratories). Images were taken on an EVOS microscope. Analysis was performed using EBImage via calculation of the percentage of pixels most positive in the FITC channel vs those in the DAPI channel.[38] Voronoi tessellation was used to identify the central peanut agglutinin-positive region of the images and quantified as percent total pixels in the image.

Frozen tissue preparation, histology, and histochemistry

The 8-μm cryosections were either fixed overnight at room temperature in Bouin solution (HT10132-1L; Sigma) and stained using Masson trichrome staining kit (HT15-1KT; Sigma) or stained with hematoxylin (GHS332; sigma) and eosin (HT110116; Sigma) for pathology. Histopathology scoring on coded sections was performed as previously described by a double-blinded researcher.[39] Trichrome images were analyzed using EBImage.[38]

Flow cytometry

Flow cytometry of organ suspensions was performed on day 49 post-BMT. For GC cells, spleens were stained with fixable-viability dye (65-0865-14 ThermoFisher), anti-CD4 (563726; BD), anti-CXCR5 (12-7185-82; eBio), anti-PD1 (63-9981-82; ThermoFisher), anti-CD19 (61-0193-82; ThermoFisher), anti-GL7 (45-5902-82 eBio), and anti-FAS (BD; 563646). Suspensions were fixed and permeabilized using a FoxP3 transcription factor staining kit (00-5523-00; eBio), intracellularly stained with anti-FoxP3 (25-5773-82; eBio) and in some studies anti-H3K27me3 (ab205728; Abcam). For plasma cell (PC) analysis, lung suspensions were stained with fixable-viability dye (65-0865-14; ThermoFisher), anti-CD38 (102718; BioLegend), anti-CD19

Figure 2. JQ1 and JQ5 impair the GC reaction in murine cGVHD/BO mice. (A-I) Transplants were performed as in Figure 1; groups are as defined in Figure 1. Results shown are pooled from 3 transplant replicates. (A-C) Flow cytometry analysis of mouse splenocytes taken 49 days posttransplant. TFH frequency is defined as % $CXCR5^+$, $PD1^+$ of $FoxP3^-$, $CD4^+$ live splenocytes. TFRs are the $CXCR5^+$, $PD1^+$ percentage of $FoxP3^+$, $CD4^+$ live splenocytes. The TFR/TFH ratio is shown. GCBs are $GL7^+$, FAS^{hi} percentage of the $CD19^+$ live splenocytes. (A) JQ5 treatment resulted in a significant decrease in TFH and GCB frequencies and increase in TFR frequency and the TFR/TFH ratio (n = 23/BM-only, n = 18/cGVHD, n = 15/JQ5). (B) Similar results are shown for each population with JQ1 treatment, consistent with reduced GC reaction (n = 14/BM-only, n = 11/cGVHD, n = 7/JQ1). (C) Representative gating for (left) TFH and TFR cells and (right) GCB cells. BM-only contours are in blue, cGVHD contours are in red. (D) Representative images of cryopreserved spleen sections stained to show GCs from mice 49 days posttransplant. Sections are stained with DAPI (blue), peanut agglutinin (PNA) rhodamine (red), and CD4 FITC (green). Images are at ×200 magnification. (E-F) (Left) Number of GCs observed in each spleen section normalized for the area of spleen in each section. A GC was counted if it was a roughly circular region of PNA^+ cells near a region of $CD4^+$ cells. Right: quantification of the average size of GCs observed in each section. The GC size was determined as the area of the PNA^+ region. For both JQ5 (E; n = 8/BM-only, n = 6/cGVHD, n = 5/JQ5) and JQ1 (F; n = 5/group), there was a significant reduction in both GC count and average size. (G) Flow cytometric analysis of single-cell lung suspensions taken from transplanted mice treated with each drug (n = 5/group). Left: total plasma cells are $CD138^+$ lymphocytes, (center) immature plasma cells are $B220^+$, $CD19^+$ plasma cells, and (right) mature plasma cells are $B220^-$, $CD19^-$ plasma cells. Results show that both drugs significantly reduced the proportion of mature plasma cells in subject lungs. (H) Mean fluorescence intensity (MFI) quantification of flow cytometry analysis of H3K27me3 content of GC cell populations gated as in panel C (n per group as in panel A). (I) Representative histograms of GCB cells H3K27me3 content for BM-only, cGVHD, and JQ5-treated mouse-derived cells. For all panels, statistics shown are results of an unpaired *t* test with Bonferroni corrected *P* values, where appropriate. $^*P < .05$, $^{**}P < .01$, $^{***}P < .001$, $^{****}P < .0001$.

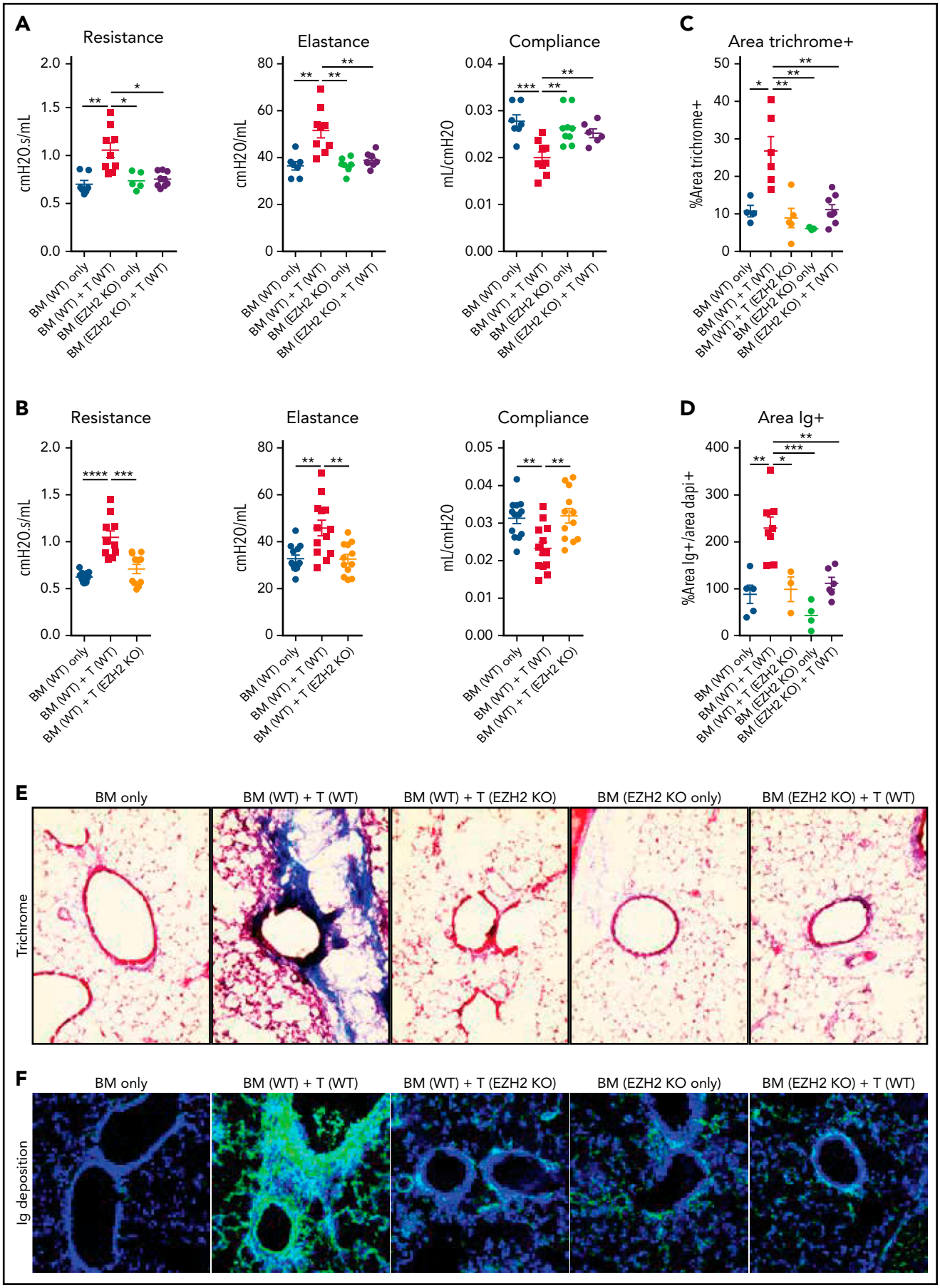

Figure 3.

(61-0193-82; ThermoFisher), and anti-B220 (562922; BD). Samples were analyzed on a BD LSRFortessa II.

RNA-sequencing sample preparation

Day 49 post-BMT spleens were homogenized, red blood cell lysed, stained for fluorescence-activated cell sorting with fixable-viability dye, anti-CD19, anti-GL7, and anti-FAS (same products as previously mentioned) and ≥100 000 cells were collected directly into an equivalent volume of Qiagen buffer RLT (74134; Qiagen) + 1% 2-ME (M6250-100ML; Sigma). Samples were frozen on dry ice until processing at the University of Minnesota Genomics Center. RNA was collected and isolates quantified by fluorometric RiboGreen assay, integrity determined using capillary electrophoresis, and samples converted to sequencing libraries using Takara Bio's SMARTer Stranded Total RNA-Seq–Pico Mammalian Kit v2 (634414).

RNA-sequencing analysis

Indexed libraries were normalized, pooled, and loaded onto a NovaSeq paired end flow cell for clustering and sequencing using Illumina's bcl2fastq v2.20. FASTQ reads were entered into the Collection of Hierarchical UMII/RIS Pipelines[40] for quality control[41]; trimming, confirming viability, and aligning reads[42] using HISAT2[43]; filtering alignments using SAMtools[44]; and generating output matrices using Subread FeatureCounts.[45] Genome alignments were run against the mm10 reference genome (GRCm38). Resulting counts were analyzed for differential gene expression using DEseq2.[46]

Results

Epigenetic modifying enzyme inhibitors to BET bromodomains or EZH2 effectively treated murine cGVHD/BO

Considering epigenetic modifying enzyme inhibitor effects on GC reactions, we investigated the BET-bromodomain inhibitor JQ1 and the novel EZH2 inhibitor JQ5 in a multiorgan cGVHD/BO model. We tested a novel EZH2 inhibitor because other commonly tested EZH2 inhibitors were ineffective in our model. UNC1999 showed toxicity (<50% survival over treatment period) (supplemental Figure 1A, available on the *Blood* Web site), whereas DZnep had no impact on the pulmonary function of treated mice (supplemental Figure 1B).[47,48]

B10.BR mice were conditioned with Cytoxan and TBI and transplanted with B6 donor BM ± a low supplemental T-cell dose (73.5×10^3). Chronic GVHD mice were treated with JQ5 (75 mg/kg JQ5), JQ1 (50 mg/kg), or vehicle intraperitoneally from days 28 to 49. Both JQ5 (Figure 1A) and JQ1 (Figure 1B) significantly ($P < .01$) improved day 49 pulmonary function across all parameters, though without significant impacts on weights or overall survival of treated mice, which is not unexpected because both weight loss and mortality are limited in this model (supplemental Figure 2).[49] The use of whole-body plethysmography to assess disease progression provides a clinically relevant functional measure of pulmonary function, above and beyond simple measures like respiratory rate, because these tests are directly analogous to the pulmonary function testing done in a clinical setting to diagnose, track, and manage BO.[50] To determine whether improvements were associated with decreased pulmonary fibrosis, lung cryosections were stained for collagen and Ig deposition. Pulmonary sections showed a significant ($P < .001$) reduction in collagen deposition in JQ5 (Figure 1C) or JQ1 (Figure 1D) treated mice compared with vehicle controls. Lung immunofluorescence staining for Ig deposition showed a near complete absence of IgG of JQ5 (Figure 1E) and JQ1 (Figure 1F) treated mice. Hematoxylin and eosin staining of other target organs, including the large intestine, liver, and spleen, showed reduced histology scores with both JQ5 and JQ1 treatment, albeit only statistically significantly in lungs (supplemental Figure 3). Together, our studies show JQ5 and JQ1 each reduced murine cGVHD/BO severity.

JQ5 and JQ1 impaired the murine cGVHD/BO GC reaction

Because BRD4 and EZH2 are upregulated in GCBs, and GCs are critical for cGVHD/BO pathogenesis, we assessed whether the observed reduction in pulmonary severity was accompanied by a GC response reduction.[16,18] For both drugs, the GC reaction was significantly ($P < .05$) inhibited, evidenced by decreased splenic TFH and GCB frequency and increased splenic T-follicular regulatory (TFR) cell frequency and TFR/TFH ratio (Figure 2A-C). Spleen cryosections were stained with rhodamine-peanut agglutinin, anti-CD4 FITC, and DAPI and images were analyzed for GC numbers per unit area in each spleen section and average size (Figure 2D). JQ5 (Figure 2E) and JQ1 (Figure 2F) showed a significantly ($P < .05$) lower GC number per mm^2 and average GC size.

To determine if the reduced GC response decreased pulmonary PC frequency of drug-treated cGVHD/BO mice, PC ($CD138^+$ lymphocytes), immature PC ($CD19^+$, $B220^+$) and mature PC ($CD19^-$, $B220^-$) frequencies were quantified. Although total lung resident PCs were largely unchanged between conditions, a significant ($P < .05$) reduction in frequency of the mature, antibody-secreting, $CD19^-$ $B220^-$ PC subpopulation was observed (Figure 2G). EZH2 inhibition by JQ5 was predicted to decrease in H3K27me3 in GC cells. Therefore, total H3K27me3 present in GC populations was

Figure 3. EZH2 expression in both donor T cells and B cells is necessary for cGVHD/BO. (A-D) Mice were transplanted as in Figure 1. Groups shown are defined by the contents of the graft given on day 0. BM (EZH2 KO) refers to T-cell-depleted BM from B6 EZH2 fl/fl CD19-Cre mice. T (EZH2 KO) refers to purified T cells from B6 EZH2 fl/fl CD4 Cre mice. Results shown are pooled from 2 transplant replicates. (A-B) Results of pulmonary function tests on mice 49 days posttransplant show significant improvement in pulmonary function if (A) BM or (B) T cells are obtained from EZH2 KO donors (n = 7/BM-only, n = 9/cGVHD, n = 7/BM [EZH2 KO] only, n = 9/BM [EZH2 KO] + T [WT], n = 6/BM [WT] + T [EZH2 KO]). (C,E) Representative images of cryopreserved lung sections from mice 49 days posttransplant (n = 4/BM-only, n = 6/cGVHD, n = 4/BM [EZH2 KO] only, n = 8/BM [EZH2 KO] + T [WT], n = 5/BM [WT] + T [EZH2 KO]). Sections were stained with Masson trichrome and analyzed for collagen deposition, which is significantly reduced in recipients of T cells or BM from EZH2 KO donors. (D,F) Representative images of cryopreserved lung sections from mice 49 days posttransplant (n = 5/BM-only, n = 8/cGVHD, n = 4/BM [EZH2 KO] only, n = 6/BM [EZH2 KO] + T [WT], n = BM [WT] + T [EZH2 KO]). Sections were stained with anti-IgG FITC and DAPI and show reduction of IgG^+ tissue in both the EZH2 KO T cell and EZH2 KO BM transplanted samples. Quantification of $FITC^+$ area is shown in panel C. All images are at ×200 magnification. Quantification of trichrome-positive area is shown in the left panel of D. Statistics shown are results of an unpaired *t* test with Bonferroni corrected *P* values when appropriate. $^*P < .05$, $^{**}P < .01$, $^{***}P < .001$, $^{****}P < .0001$. KO, knockout.

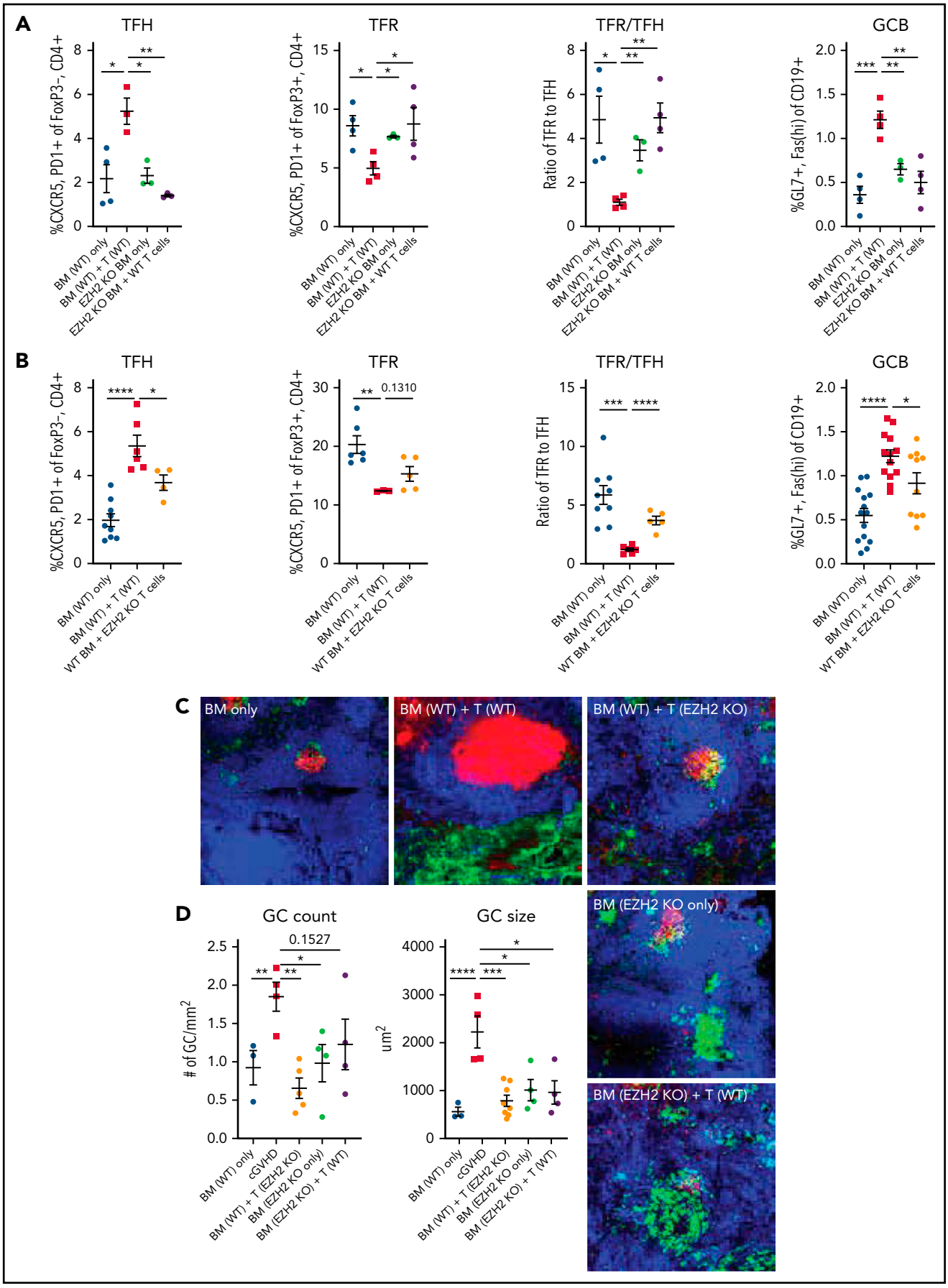

Figure 4.

quantified. JQ5- vs vehicle-treated mice had significantly reduced H3K27me3 in TFH, TFR, and GCB cells (Figure 2H-I).

EZH2 expression is necessary in donor BM and T cells for murine cGVHD/BO and GC responses

Because EZH2 is upregulated in T cells and B cells in GCs that play a significant role in cGVHD pathogenesis,[15,16,36,51] EZH2 was selectively deleted in donor T cells that give rise to TFHs or BM B cells that produce GCBs. B10.BR recipients were transplanted with wild-type (WT) B6 or EZH2 knockout (ko) BM from EZH2 fl/fl CD19 Cre donors ± purified WT B6 T cells. On day 49 we observed significant ($P < .05$) improvement in pulmonary function in recipients of EZH2 fl/fl CD19 Cre vs WT BM (Figure 3A). To assess EZH2 effects in donor T cells, mice were given WT B6 BM + WT or EZH2 fl/fl CD4 Cre T cells. Mice receiving EZH2 ko T cells showed significant ($P < .01$) improvement in pulmonary function (Figure 3B). Recipients of EZH2 ko T cells or EZH2 ko BM cells had a significant reduction in lung collagen (Figure 3C,F) and IgG deposition (Figure 3D-E).

Next, we sought to determine if EZH2 expression was required in GCBs to mediate murine cGVHD/BO. Mice transplanted with B6 donor EZH2 fl/fl CD19 Cre BM + WT T cells had a significant ($P < .05$) reduction TFHs and GCBs along with an increase in TFR and TFR/TFH ratio, implicating EZH2 expression in GCBs as a key regulator of the GC response (Figure 4A). Mice transplanted with B6 donor WT BM + EZH2 fl/fl × CD4-Cre T cells had a significant ($P < .05$) reduction TFHs and GCBs and an increased TFR/TFH ratio. Tissue analyses paralleled immune analyses (Figure 4). Recipients of WT BM + EZH2 fl/fl × CD4-Cre vs WT T cells had significantly reduced GC numbers and size (Figure 4D). GC size also was reduced in recipients of EZH2 fl/fl × CD19-Cre vs WT BM + WT T cells. Together, these findings demonstrate that donor TFH and GCB cell EZH2 expression in donor TFHs and GCBs is essential for cGVHD/BO pathogenesis.

JQ5 but not JQ1 slows the progression of murine sclerodermatous cGVHD

To determine whether JQ5 or JQ1 could attenuate skin fibrosis in a murine sclerodermatous cGVHD model, B10.D2 BM and T cells were transplanted into minor histocompatibility antigen-disparate irradiated BALB/c recipients and monitored twice weekly for clinical and skin scores. Treatment was initiated after the average clinical scores were >1 (day 20) and continued throughout study duration. Clinical scores were significantly lower within 20 days and skin scores within 10 days of JQ5 treatment vs vehicle controls (Figure 5A) without survival or weight improvement. In contrast, JQ1 did not reduce cutaneous disease severity and proved toxic to transplanted mice, with accelerated weight loss and mortality within 2 weeks of initiating JQ1 treatment (Figure 5B). Day 45 images of JQ5-treated mice showed fewer and less severe skin lesions with JQ5, whereas day 28 images of JQ1-treated mice did not ameliorate sclerodermatous cGVHD (Figure 5C).

Previously, we reported that sclerodermatous cGVHD is Stat3-dependent and splenic T cells isolated from mice expressed the interferon-γ (IFN-γ) and the Stat3-dependent cytokine IL17.[35] Inflammatory cytokine production measured in lymph node-derived T cells at study termination revealed JQ5 treatment significantly ($P < .05$) reduced IL-17 and IFN-γ producing $CD4^+$ T-cell frequency (Figure 5D). Skin cryosections showed significantly diminished collagen deposition in the skin of JQ5 vs vehicle-treated mice (Figure 5E-F). Together, these findings suggest that JQ5 has treatment potential for multiple cGVHD manifestations, whereas JQ1's potential appears limited to management of cGVHD/BO and not scleroderma.

JQ5 and JQ1 induce distinct transcriptional signatures in GCBs

JQ1 and JQ5 each were effective in cGVHD/BO, whereas only JQ5 was effective in sclerodermatous cGVHD. To investigate the mechanistic targets of each drug, we sequenced the RNA of GCBs isolated from the spleens of cGVHD/BO mice 49 days post-transplant. After alignment and quantification, principal component analysis was used to cluster samples. By limiting variance to the top 500 genes, principal component analysis clustering cleanly segregated the different treatment conditions while explaining nearly one-half of the total variance in the dataset. Interestingly, neither JQ1 nor JQ5 coclustered with BM-only samples, whereas JQ1 clustered close to cGVHD (Figure 6A), suggesting that neither drug restored cGVHD GCBs to the state of BM-only transplanted mice. This is further evident in differential gene expression analysis. Each agent induced differentially significant (adjusted P value $< .05$, $\log_2$ fold change >0.15) changes in a relatively small number of genes (JQ1 [40] and JQ5 [27]) (Figure 6B-C), the vast majority of which did not overlap with other treatment conditions (Figure 6D). Although neither drug reverted the GCB transcriptome to a healthy BM-only–like state, each drug imposed different changes in GCBs in cGVHD.

To determine how genetic processes involved in cGVHD/BO were affected, we performed gene set enrichment analysis using the molecular signatures database (MsigDB) hallmark gene collections.[52] The resulting network map of enriched gene sets in the BM-only vs cGVHD comparison demonstrated that multiple inflammatory signaling cascades (IFN-γ inflammatory response and TNF-α signaling) were enriched in cGVHD-derived GCBs. In contrast, proproliferative gene sets (mTORC1 signaling and Myc targets) were enriched in GCBs of BM-only transplanted mice (Figure 6E). These proproliferative pathways were similarly enriched in JQ5-treated samples. In contrast, these pathways

Figure 4. In BO cGVHD EZH2 is necessary for the GC reaction. (A-D) Transplants were performed as in Figure 1; groups are as defined in Figure 3. (A-B) Flow cytometry analysis of mouse splenocytes taken 49 days posttransplant. Cell populations for flow cytometry analysis are as defined in Figure 2. Results show that when EZH2 is knocked out in both the BM compartment (A) (n = 4/group) and T-cell compartment (B) (n = 14/BM-only, n = 13/cGVHD, n = 10/BM [WT] + T [EZH2 KO]) of the graft, there is a significant reduction in the TFH and GCB frequencies and a significant increase in the TFR/TFH ratio. (C) Representative images of cryopreserved spleen sections stained to show GCs from mice 49 days posttransplant. Sections are stained with DAPI (blue), PNA rhodamine (red), and CD4 FITC (green). Images are ×200 magnification. (D) Left panel shows the number of GCs observed in each spleen section normalized for the area of spleen in each section. Right panel is a quantification of the average size of GCs observed in each section. GCs were identified and quantified as in Figure 2. Quantification shows when EZH2 is knocked out in either the BM and T-cell compartments, there is a comparable reduction in both the GC count and average size. N = 8/BM-only, n = 6/cGVHD, n = 5/BM (EZH2 KO) only, n = 4/BM (EZH2 KO) + T (WT), n = 4/BM (WT) + T (EZH2 KO). For all panels, statistics shown are results of an unpaired t test with Bonferroni corrected P values, where appropriate. *$P < .05$, **$P < .01$, ***$P < .001$, ****$P < .0001$.

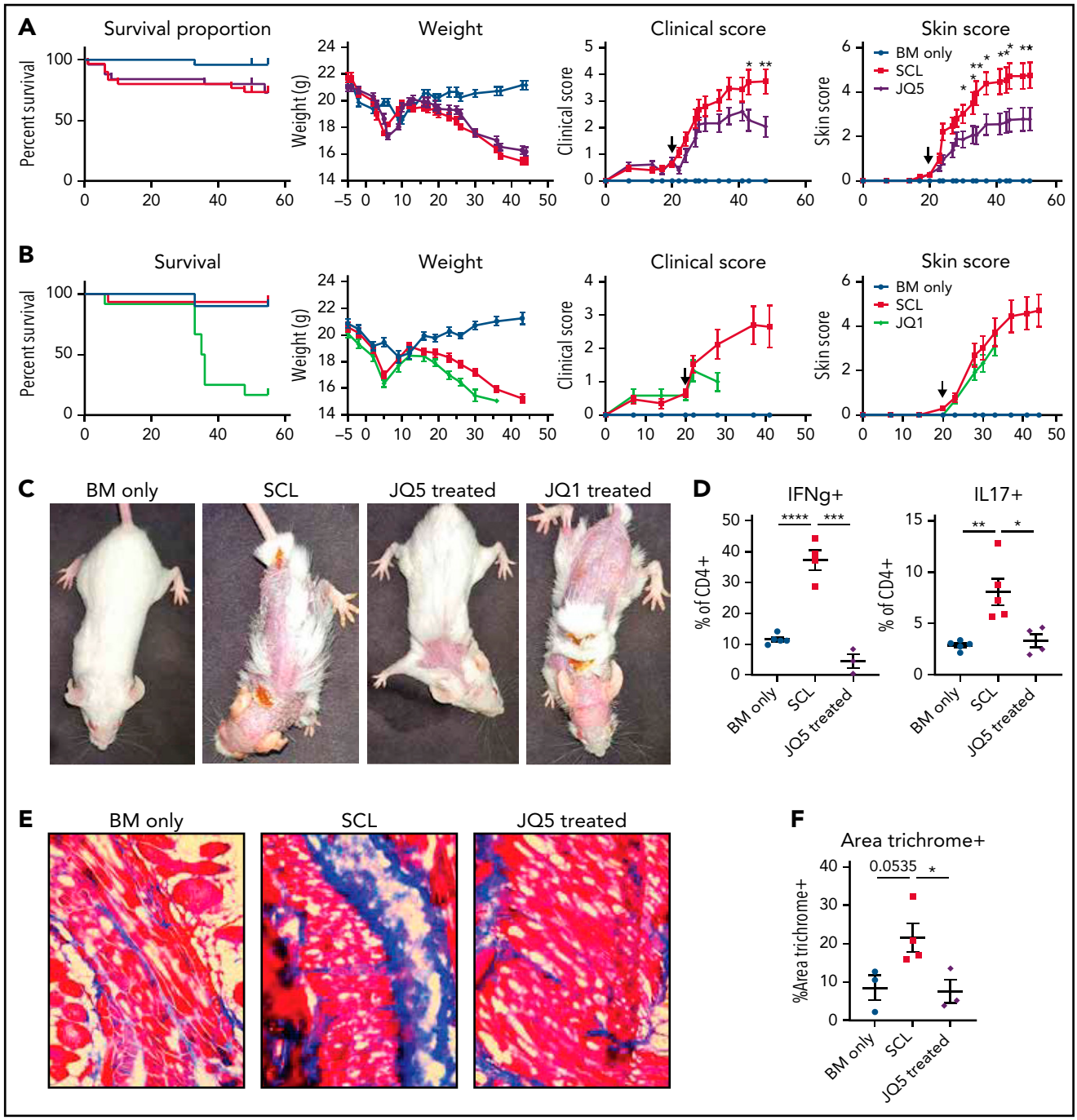

Figure 5. Treatment with JQ5, but not JQ1, can treat sclerodermatous cGVHD. (A-C) BALB/c mice were given TBI (700 cGy on day −1) followed by infusion of 10^7 B10.D2 BM ± 1.8×10^6 CD4 and 0.9×10^6 CD8 T cells (day 0). JQ5- and JQ1-treated mice received treatment as in Figure 1 from days 20 to 45 posttransplant, n = 25/group. (A-B) From left to right, graphs show impact of JQ5 treatment on recipient survival, mean weights, clinical scores, and skin scores. Arrows on clinical and skin score plots indicate time of treatment initiation. (A) Although JQ5 did not significantly improve either weights or survival proportion, treated mice showed significantly reduced clinical scores, and skin scores as early as 10 days after initial treatment. (B) JQ1 treatment shows evidence of toxicity within 7 days of beginning therapy with no mice surviving beyond 2 weeks after treatment initiation. (C) Representative images of sclerodermatous mice with or without treatment with each drug. Images taken 45 days posttransplant, except for JQ1-treated mouse, where image was taken 34 days posttransplant. (D) Flow cytometry analysis of cytokine production from transplanted mouse lymph nodes shows a significant reduction in inflammatory cytokine production with JQ5 treatment, indicative of reduced disease, n = 5 per group. (E) Representative images of cryopreserved skin cross sections from mice 45 days posttransplant. Sections were stained with Masson trichrome. Images are ×200 magnification. (F) Quantification of trichrome$^+$ area of skin cross sections in panel C shows a significant reduction in trichrome-positive area with JQ5 treatment, n = 4 per group. This correlates to a reduction in skin collagen deposition with treatment. *$P < .05$, **$P < .01$, ***$P < .001$, ****$P < .0001$.

were enriched in cGVHD compared with JQ1-treated samples, indicating JQ1 did not increase proproliferative pathway expression the way JQ5 did (Figure 6F,H). With respect to the immune signaling pathways associated with cGVHD, both JQ5 and JQ1 reduced pathway enrichment (Figure 6G-H). Together, these findings suggest that although neither drug restored GCBs to a

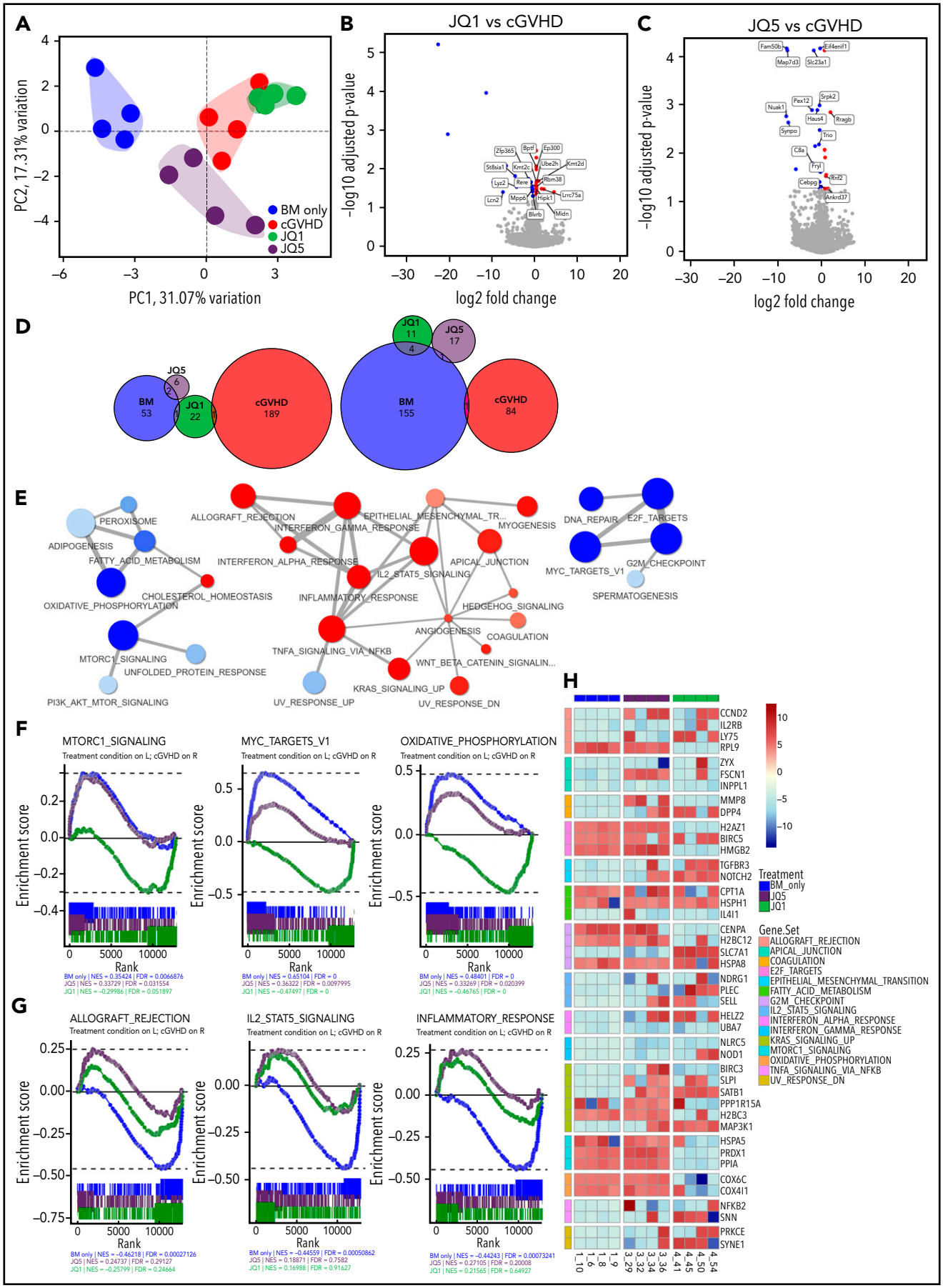

Figure 6.

BM-only like transcriptome, immune signaling disruption in cGVHD GCBs provides a likely mechanism by which both drugs contribute to GC response impairment in cGVHD/BO mice, whereas JQ5 but not JQ1 restores proproliferative pathways closer to that observed in BM-Only GCBs.

Discussion

Here, we demonstrated that small molecule inhibitors of epigenetic modifiers can disrupt the GC response and ameliorate cGVHD/BO. Within these findings, we have expanded on the promise of JQ1 demonstrating that although it may not be effective in all models, JQ1 treatment can ablate pulmonary dysfunction in cGVHD/BO. More critically, we present the first in vivo therapeutic studies of the novel EZH2 inhibitor JQ5, which was able to reduce cGVHD incidence in both a BO and sclerodermatous murine model. Although previous studies have investigated both EZH2 inhibition and BET bromodomain inhibition in aGVHD, aGVHD and cGVHD have independent and significantly different underlying mechanisms and pathophysiology.[53] Research into the roles of these inhibitors as treatments for aGVHD has limited bearing on their impact in cGVHD. Furthermore, in aGVHD, the mechanistic data on these types of inhibitors largely focused on their impacts to T-cell apoptosis and how that can affect disease.[32,54] By contrast, our studies focus on the role of EZH2 and BET inhibitors on the GC reaction. These key differences speak to the novelty of these findings and their potential impact.

Chromatin-modifying protein inhibitors have gained traction in the field of cancer treatment research; they are used to target the aberrant epigenetic landscape unique to cancer cells.[55] Our findings expand the scope of these drugs by demonstrating their potential impact in transplant biology,[29] and the proposition that misregulated biological processes in which their target enzymes are involved can be disrupted.[56-60] Previous work on epigenetic targeting therapies in GVHD have shown that the DNA methyltransferase inhibitor azacytidine was able to reduce GVHD in both murine and xenogeneic models.[61,62] Most notably, the histone deacetylase inhibitor vorinostat has shown success in a phase 2 clinical trial for aGVHD prevention.[63] Vorinostat and azacytidine supported T-regulatory cell expansion, and vorinostat additionally suppressed host antigen-presenting cells and reduced T helper 1 (Th1) and Th17 cells in aGVHD models.[62,64-66] In contrast to these earlier reports, we expand this strategy into cGVHD, looking at both a separate mechanism, the germinal center, and 2 epigenetic modifications (H3K27Ac recognition, H3K27me3 regulation) that have not been extensively studied in cGVHD.

Of the JQ5 inhibitors that we tested, only JQ5 was able to successfully treat murine cGVHD. In contrast, UNC1999 was highly toxic, with 50% of treated mice dying within 2 days of initiating therapy, whereas DZNep had no observed impact on pulmonary function. These results are similar to what is observed in aGVHD models, where the EZH2 inhibitors GSK126 and EPZ6438, which specifically decrease H3K27me3 without affecting EZH2 protein, failed to prevent aGVHD, even though EZH2 genetic ablation in donor T cells reduced aGVHD severity.[67,68] This makes JQ5 uniquely able to recapitulate the improvements observed in EZH2 knockout models, likely as a result of the compound specificity and mechanism. Unlike JQ5, which is highly specific to EZH2 and a direct competitive inhibitor for the binding of *S*-adenosyl-methionine,[69] DZNep impairs EZH2 indirectly by inhibiting AdoHcy cyclase to reduce the availability of SAM.[48,70] Although UNC1999 is also an inhibitor of the binding of *S*-adenosyl-methionine, it lacks the high specificity for EZH2 of JQ5.[47]

Both JQ1 and JQ5 successfully reduced the splenic frequency of GC cell populations, as well the GC frequency and size, correlating with a clear improvement in pulmonary function and adding to a growing body of evidence that the GC reaction plays a key role in the pathogenesis of cGVHD/BO generated under the conditions detailed here. By demonstrating that both drugs also reduced mature PC lung infiltration, a previously uninvestigated component of this mechanism, implicates PCs as potential contributors to cGVHD/BO pathogenesis. Other examples of successful preclinical drugs that treated murine cGVHD while impairing the GC response include pirfenidone (5-methyl-1-phenyl-2-[^{1}H]-pyridone; SMAD2/3 inhibitor), ibrutinib (anti-Bruton tyrosine kinase/ITK monoclonal antibody), and Bcl-6 peptidomimetic inhibitor 79-6.[71-73]

In a high inflammatory sclerodermatous cGVHD model, JQ5 treatment reduced the formation of skin lesion in treated animals. Contrasting with its response in the cGVHD/BO model, JQ1 treatment proved toxic in this sclerodermatous model. We propose that JQ1 is not well tolerated under high inflammatory conditions as seen in the sclerodermatous model and in contrast to the low inflammatory conditions cGVHD/BO GVHD model. In support of that contention, we also tested the impact of JQ1 on an actual aGVHD model and observed accelerated lethality (data not shown).

Previous mechanistic insights from sequencing experiments on cGVHD are scarce. Although some single-cell capture and sequencing of samples from patients with cGVHD has been performed, the emphasis has largely been on T cells and is limited to circulating cells.[74-76] Previous murine studies also focused primarily on the T-cell population in cGVHD.[77,78] Here, we report the first detailed immune analyses coupled with transcriptomic in GCBs

Figure 6. JQ5 and JQ1 impair GCB cells through distinct transcriptomic signatures. All results from analysis of sorted GCBs collected ~49 days posttransplant in cGVHD/BO B6→B10.BR model. Four samples in each group are used for analysis; samples were chosen to be most representative of each treatment condition by pulmonary function test results. (A) Principal component analysis (PCA) of top 4 samples in each treatment condition, calculated with top 500 most variable genes. Treatment condition variation along the top 2 PCAs explains ~48% of variance within the dataset. All groups cluster independently. (B-C) Volcano plot of differentially expressed genes in either (A) JQ1- or (B) JQ5-treated samples against vehicle-treated (cGVHD) samples. Differentially expressed genes called as having an adjusted value of $P < .05$, and a $\log_2$ fold change greater than 0.15. Twenty-four genes were differentially increased and 16 were reduced with JQ1, and 8 genes were differentially increased and 19 were reduced with JQ5. (D) Euler plots of overlapping differentially expressed genes in each of the 4 treatment conditions. Left plot is upregulated genes, whereas right is downregulated genes. (E) Gene set enrichment analysis (GSEA) network mapping of MsigDB hallmark gene sets in BM-only vs cGVHD comparison. Red nodes were increased with cGVHD vs BM-only samples, blue nodes were decreased. (F-G) Individual enrichment barcode plots for (F, left to right) MTORC1 signaling, Myc targets V1, oxidative phosphorylation; (G; left to right) allograft rejection, IL2-STAT5 signaling, and inflammatory response hallmark gene sets. On all plots, genes enriched in the treatment condition are on the left, whereas genes enriched in cGVHD are on the right. Gene sets in panel E JQ5 and JQ1 impacted enrichment differently, gene sets in panel F sets were enriched comparably. (H) Heatmap of high variance genes in major GSEA nodes described in panel D. Colors are blue for BM only, red for cGVHD, purple for JQ5 treated, and green for JQ1 treated (A,C,F-G).

from cGVHD/BO mice. Interestingly, neither compound restored a BM-only (non-cGVHD control) transcriptomic state. Rather, each compound induced a unique set of changes independently incompatible with GCB function in cGVHD. Decreased proproliferative signaling expression in cGVHD relative to BM-only GCBs is at first counterintuitive because these pathways are essential for GC formation.[79] However, these findings may be a sign of active somatic hypermutation or class switch recombination in cGVHD GCBs, processes that can decrease proliferative signaling, consistent with elevated immune signaling observed in our analysis.[79,80] Both JQ5 and JQ1 lead to a reduction in the enrichment of several immune signaling pathways, especially IL2-STAT5 signaling and the inflammatory response, suggesting that these and not proproliferative pathways are critical for GC formation in cGVHD/BO mice. JQ1 did not impact genes associated with proliferation such as mTORC1 signaling and cMyc targets, providing some mechanistic insight into the different effects each drug has.

Taken together, our results demonstrate the efficacy of targeted inhibition of epigenetic targets as a strategy for the treatment of cGVHD. Both the novel EZH2 inhibitor JQ5 and BET-bromodomain inhibitor JQ1 reduced the severity of pulmonary fibrosis from cGVHD/BO. Despite the distinct molecular mechanisms altered by JQ5 vs JQ1, each disrupted the GC reaction and reduced disease severity. Because existing options for treatment of cGVHD remain limited, these studies provide a strong rational for future clinical investigation of bromodomain inhibitors and EZH2 inhibitors for treatment of cGVHD/BO (and of EZH2 inhibitors for the treatment of sclerodermatous cGVHD) as both types of compounds are either in clinical trial or approved by the FDA.

Acknowledgments

This work was supported, in part, by National Institutes of Health, National Cancer Institute (P01 CA142106), National Institute of Allergy and Infectious Disease (P01 AI56299, T32 AI007313, and R01 CA222218), Leukemia Society of America Translational Research Grant 6458-15, and the Children's' Cancer Research Fund.

Authorship

Contribution: M.C.Z. designed experiments, performed experiments, and wrote the paper; R.F. designed and performed experiments; K.G.P., S.Y.R., S.J., F.A.M., A.S., and G.T. performed and assisted with experiments; P.M.C.P., M.L.H., P.T.S., and L.S.K. assisted with bioinformatic analyses; J.Q. and J.E.B. synthesized and provided reagents and discussed experiments; J.A.B. and M.D. provided mice for experiments; A.P.-M. provided histopathological scoring and edited and approved the manuscript; A.H.S., C.S.C., J.K., J.H.A., R.J.S., J.R., L.L., I.M., G.R.H., K.P.A.M., D.H.M., J.S.S., W.J.M., and Y.Z. discussed experiments, results, and conclusions; J.Q. and B.R.B. designed experiments, reviewed data, and assisted in manuscript preparation; and all authors edited the manuscript.

Conflict-of-interest disclosure: B.R.B. receives remuneration as an advisor to Magenta Therapeutics and BlueRock Therapeutics; research funding from BlueRock Therapeutics, Rheos Medicines, Equilibre biopharmaceuticals, and Carisma Therapeutics, Inc.; and is a cofounder of Tmunity Therapeutics. J.Q. is a scientific cofounder and consultant for Epiphanes and a consultant for Talus. G.R.H. has consulted for Generon Corporation, NapaJen Pharma, iTeos Therapeutics, and Neoleukin Therapeutics and has received research funding from Compass Therapeutics, Syndax Pharmaceuticals, Applied Molecular Transport, Serplus Technology, Heat Biologics, Laevoroc Oncology, and iTeos Therapeutics. The remaining authors declare no competing financial interests.

The current affiliation for J.E.B. is Novartis Institute of Biomedical Research, Cambridge, MA.

ORCID profiles: M.C.Z., 0000-0001-6971-3170; S.J., 0000-0001-6504-3640; F.A.M., 0000-0003-4270-8560; M.D., 0000-0002-1479-9840; J.R., 0000-0001-5526-4669; J.Q., 0000-0002-1461-3356; B.R.B., 0000-0002-9608-9841.

Correspondence: Bruce R. Blazar, MMC 366, University of Minnesota, 420 Delaware St SE, Minneapolis, MN 55455; e-mail: blaza001@umn.edu; and Jun Qi, Department of Cancer Biology, Dana-Farber Cancer Institute, Harvard Medical School, 450 Brookline Ave LC-2210, Boston, MA 02215; e-mail: jun_qi@dcfi.harvard.edu.

Footnotes

Submitted 25 October 2021; accepted 9 February 2022; prepublished online on *Blood* First Edition 28 February 2022. DOI 10.1182/blood.2021014557.

Data can be found at accession number PRJNA773813.

The online version of this article contains a data supplement.

There is a *Blood* Commentary on this article in this issue.

The publication costs of this article were defrayed in part by page charge payment. Therefore, and solely to indicate this fact, this article is hereby marked "advertisement" in accordance with 18 USC section 1734.

REFERENCES

1. Greinix HT. Chronic GVHD: progress in salvage treatment? *Blood*. 2017;130(21):2237-2238.
2. Flowers MED, Parker PM, Johnston LJ, et al. Comparison of chronic graft-versus-host disease after transplantation of peripheral blood stem cells versus bone marrow in allogeneic recipients: long-term follow-up of a randomized trial. *Blood*. 2002;100(2):415-419.
3. Lee SJ. Have we made progress in the management of chronic graft-vs-host disease? *Best Pract Res Clin Haematol*. 2010;23(4):529-535.
4. Socié G, Stone JV, Wingard JR, et al; Late Effects Working Committee of the International Bone Marrow Transplant Registry. Long-term survival and late deaths after allogeneic bone marrow transplantation. *N Engl J Med*. 1999;341(1):14-21.
5. Lee SJ, Klein JP, Barrett AJ, et al. Severity of chronic graft-versus-host disease: association with treatment-related mortality and relapse. *Blood*. 2002;100(2):406-414.
6. Miklos D, Cutler CS, Arora M, et al. Ibrutinib for chronic graft-versus-host disease after failure of prior therapy. *Blood*. 2017;130(21):2243-2250.
7. Wolff D, Gerbitz A, Ayuk F, et al. Consensus conference on clinical practice in chronic graft-versus-host disease (GVHD): first-line and topical treatment of chronic GVHD. *Biol Blood Marrow Transplant*. 2010;16(12):1611-1628.
8. Jagasia M, Lazaryan A, Bachier CR, et al. ROCK2 inhibition with belumosudil (KD025) for the treatment of chronic graft-versus-host disease. *J Clin Oncol*. 2021;39(17):1888-1898.
9. Zeiser R, Polverelli N, Ram R, et al; REACH3 Investigators. Ruxolitinib for glucocorticoid-refractory chronic graft-versus-host disease. *N Engl J Med*. 2021;385(3):228-238.
10. Mawardi H, Hashmi SK, Elad S, Aljurf M, Treister N. Chronic graft-versus-host disease: current management paradigm and future perspectives. *Oral Dis*. 2019;25(4):931-948.
11. Hildebrandt GC, Fazekas T, Lawitschka A, et al. Diagnosis and treatment of pulmonary chronic GVHD: report from the consensus conference on clinical practice in chronic GVHD. *Bone Marrow Transplant*. 2011;46(10):1283-1295.

12. Flynn R, Paz K, Du J, et al. Targeted Rho-associated kinase 2 inhibition suppresses murine and human chronic GVHD through a Stat3-dependent mechanism. *Blood*. 2016; 127(17):2144-2154.

13. Jagasia M, Salhotra A, Bachier CR, et al. KD025-208: a phase 2a study of KD025 for patients with chronic graft versus host disease (cGVHD) – pharmacodynamics (PD) and updated results. *Blood*. 2018; 132(suppl 1):602.

14. Panoskaltsis-Mortari A, Tram KV, Price AP, Wendt CH, Blazar BR. A new murine model for bronchiolitis obliterans post-bone marrow transplant. *Am J Respir Crit Care Med*. 2007;176(7):713-723.

15. Srinivasan M, Flynn R, Price A, et al. Donor B-cell alloantibody deposition and germinal center formation are required for the development of murine chronic GVHD and bronchiolitis obliterans. *Blood*. 2012;119(6):1570-1580.

16. Flynn R, Du J, Veenstra RG, et al. Increased T follicular helper cells and germinal center B cells are required for cGVHD and bronchiolitis obliterans. *Blood*. 2014;123(25): 3988-3998.

17. Béguelin W, Popovic R, Teater M, et al. EZH2 is required for germinal center formation and somatic EZH2 mutations promote lymphoid transformation. *Cancer Cell*. 2013;23(5):677-692.

18. Velichutina I, Shaknovich R, Geng H, et al. EZH2-mediated epigenetic silencing in germinal center B cells contributes to proliferation and lymphomagenesis. *Blood*. 2010;116(24):5247-5255.

19. Czermin B, Melfi R, McCabe D, Seitz V, Imhof A, Pirrotta V. Drosophila enhancer of Zeste/ESC complexes have a histone H3 methyltransferase activity that marks chromosomal Polycomb sites. *Cell*. 2002; 111(2):185-196.

20. Cao R, Wang L, Wang H, et al. Role of histone H3 lysine 27 methylation in Polycomb-group silencing. *Science*. 2002; 298(5595):1039-1043.

21. Boyer LA, Plath K, Zeitlinger J, et al. Polycomb complexes repress developmental regulators in murine embryonic stem cells. *Nature*. 2006;441(7091):349-353.

22. Lee TI, Jenner RG, Boyer LA, et al. Control of developmental regulators by Polycomb in human embryonic stem cells. *Cell*. 2006; 125(2):301-313.

23. Bernstein BE, Mikkelsen TS, Xie X, et al. A bivalent chromatin structure marks key developmental genes in embryonic stem cells. *Cell*. 2006;125(2):315-326.

24. Shin DM, Liu R, Wu W, et al. Global gene expression analysis of very small embryonic-like stem cells reveals that the Ezh2-dependent bivalent domain mechanism contributes to their pluripotent state. *Stem Cells Dev*. 2012; 21(10):1639-1652.

25. Li B, Chng WJ. EZH2 abnormalities in lymphoid malignancies: underlying mechanisms and therapeutic implications. *J Hematol Oncol*. 2019;12(1):118.

26. Villanueva MT. Anticancer drugs: all roads lead to EZH2 inhibition. *Nat Rev Drug Discov*. 2017;16(4):239.

27. Tan JZ, Yan Y, Wang XX, Jiang Y, Xu HE. EZH2: biology, disease, and structure-based drug discovery. *Acta Pharmacol Sin*. 2014; 35(2):161-174.

28. Filippakopoulos P, Qi J, Picaud S, et al. Selective inhibition of BET bromodomains. *Nature*. 2010;468(7327):1067-1073.

29. Alqahtani A, Choucair K, Ashraf M, et al. Bromodomain and extra-terminal motif inhibitors: a review of preclinical and clinical advances in cancer therapy. *Future Sci OA*. 2019;5(3):FSO372.

30. Mele DA, Salmeron A, Ghosh S, Huang HR, Bryant BM, Lora JM. BET bromodomain inhibition suppresses TH17-mediated pathology. *J Exp Med*. 2013;210(11):2181-2190.

31. Gao F, Yang Y, Wang Z, Gao X, Zheng B. BRAD4 plays a critical role in germinal center response by regulating Bcl-6 and NF-κB activation. *Cell Immunol*. 2015;294(1): 1-8.

32. Sun Y, Wang Y, Toubai T, et al. BET bromodomain inhibition suppresses graft-versus-host disease after allogeneic bone marrow transplantation in mice. *Blood*. 2015; 125(17):2724-2728.

33. Wang D, Quiros J, Mahuron K, et al. Targeting EZH2 reprograms intratumoral regulatory T cells to enhance cancer immunity. *Cell Rep*. 2018;23(11):3262-3274.

34. DuPage M, Chopra G, Quiros J, et al. The chromatin-modifying enzyme Ezh2 is critical for the maintenance of regulatory T cell identity after activation. *Immunity*. 2015; 42(2):227-238.

35. Radojcic V, Pletneva MA, Yen H-R, et al. STAT3 signaling in $CD4^+$ T cells is critical for the pathogenesis of chronic sclerodermatous graft-versus-host disease in a murine model. *J Immunol*. 2010;184(2):764-774.

36. Anderson BE, McNiff J, Yan J, et al. Memory $CD4^+$ T cells do not induce graft-versus-host disease. *J Clin Invest*. 2003;112(1): 101-108.

37. Zhang H, Qi J, Reyes JM, et al. Oncogenic deregulation of EZH2 as an opportunity for targeted therapy in lung cancer. *Cancer Discov*. 2016;6(9):1006-1021.

38. Pau G, Fuchs F, Sklyar O, Boutros M, Huber W. EBImage – an R package for image processing with applications to cellular phenotypes. *Bioinformatics*. 2010;26(7):979-981.

39. Blazar BR, Taylor PA, McElmurry R, et al. Engraftment of severe combined immune deficient mice receiving allogeneic bone marrow via in utero or postnatal transfer. *Blood*. 1998;92(10):3949-3959.

40. Baller J, Kono T, Herman A, Zhang YCURP. A lightweight CLI framework to enable novice users to analyze sequencing datasets in parallel. *ACM International Conference Proceeding Series*. 2019.

41. Anders S. Babraham bioinformatics. FastQC: a quality control tool for high throughput sequence data. *Soil (Gottingen)*. 2010;5(1).

42. Bolger AM, Lohse M, Usadel B. Trimmomatic: a flexible trimmer for Illumina sequence data. *Bioinformatics*. 2014;30(15): 2114-2120.

43. Kim D, Paggi JM, Park C, Bennett C, Salzberg SL. Graph-based genome alignment and genotyping with HISAT2 and HISAT-genotype. Nat Biotechnol. 2019; 37(8):907-915.

44. Danecek P, Bonfield JK, Liddle J, et al. Twelve years of SAMtools and BCFtools. *Gigascience*. 2021;10(2):giab008.

45. Liao Y, Smyth GK, Shi W. featureCounts: an efficient general purpose program for assigning sequence reads to genomic features. *Bioinformatics*. 2014;30(7):923-930.

46. Love MI, Huber W, Anders S. Moderated estimation of fold change and dispersion for RNA-seq data with DESeq2. *Genome Biol*. 2014;15(12):550.

47. Konze KD, Ma A, Li F, et al. An orally bioavailable chemical probe of the lysine methyltransferases EZH2 and EZH1. *ACS Chem Biol*. 2013;8(6):1324-1334.

48. Miranda TB, Cortez CC, Yoo CB, et al. DZNep is a global histone methylation inhibitor that reactivates developmental genes not silenced by DNA methylation. *Mol Cancer Ther*. 2009;8(6):1579-1588.

49. Sinha RK, Flynn R, Zaiken M, et al. Activated protein C ameliorates chronic graft-versus-host disease by PAR1-dependent biased cell signaling on T cells. *Blood*. 2019;134(9): 776-781.

50. Reynaud-Gaubert M, Thomas P, Badier M, et al. Early detection of airway involvement in obliterative bronchiolitis after lung transplantation. *Am J Respir Crit Care Med*. 2012;161(6):1924-1929.

51. Sarantopoulos S, Blazar BR, Cutler C, Ritz J. B cells in chronic graft-versus-host disease. *Biol Blood Marrow Transplant*. 2015;21(1): 16-23.

52. Liberzon A, Birger C, Thorvaldsdóttir H, Ghandi M, Mesirov JP, Tamayo P. The Molecular Signatures Database (MSigDB) hallmark gene set collection. *Cell Syst*. 2015; 1(6):417-425.

53. Blazar BR, Murphy WJ, Abedi M. Advances in graft-versus-host disease biology and therapy. *Nat Rev Immunol*. 2012;12(6): 443-458.

54. Kamijo H, Sugaya M, Takahashi N, et al. BET bromodomain inhibitor JQ1 decreases CD30 and CCR4 expression and proliferation of cutaneous T-cell lymphoma cell lines. *Arch Dermatol Res*. 2017;309(6):491-497.

55. Berdasco M, Esteller M. Aberrant epigenetic landscape in cancer: how cellular identity goes awry. *Dev Cell*. 2010;19(5):698-711.

56. Chen H, Liu H, Qing G. Targeting oncogenic Myc as a strategy for cancer treatment. *Signal Transduct Target Ther*. 2018;3(1):5.

57. Mertz JA, Conery AR, Bryant BM, et al. Targeting MYC dependence in cancer by inhibiting BET bromodomains. *Proc Natl Acad Sci USA*. 2011;108(40):16669-16674.

58. Zuber J, Shi J, Wang E, et al. RNAi screen identifies Brd4 as a therapeutic target in acute myeloid leukaemia. *Nature*. 2011; 478(7370):524-528.

59. Stewart HJS, Horne GA, Bastow S, Chevassut TJT. BRD4 associates with p53 in DNMT3A-mutated leukemia cells and is implicated in apoptosis by the bromodomain inhibitor JQ1. *Cancer Med*. 2013;2(6): 826-835.

60. Dawson MA, Prinjha RK, Dittmann A, et al. Inhibition of BET recruitment to chromatin as an effective treatment for MLL-fusion leukaemia. *Nature*. 2011;478(7370):529-533.

61. Ehx G, Fransolet G, de Leval L, et al. Azacytidine prevents experimental xenogeneic graft-versus-host disease without abrogating graft-versus-leukemia effects. *OncoImmunology*. 2017;6(5): e1314425.

62. Cooper ML, Choi J, Karpova D, et al. Azacitidine mitigates graft-versus-host disease via differential effects on the proliferation of T effectors and natural regulatory T cells in vivo. *J Immunol*. 2017; 198(9):3746-3754.

63. Choi SW, Braun T, Henig I, et al. Vorinostat plus tacrolimus/methotrexate to prevent GVHD after myeloablative conditioning, unrelated donor HCT. *Blood*. 2017;130(15): 1760-1767.

64. Holtan SG, Weisdorf DJ. Vorinostat is victorious in GVHD prevention. *Blood*. 2017; 130(15):1690-1691.

65. Choi S, Reddy P. HDAC inhibition and graft versus host disease. *Mol Med*. 2011;17(5-6): 404-416.

66. Reddy P, Maeda Y, Hotary K, et al. Histone deacetylase inhibitor suberoylanilide hydroxamic acid reduces acute graft-versus-host disease and preserves graft-versus-leukemia effect. *Proc Natl Acad Sci USA*. 2004;101(11):3921-3926.

67. Huang Q, He S, Tian Y, et al. Hsp90 inhibition destabilizes Ezh2 protein in alloreactive T cells and reduces graft-versus-host disease in mice. *Blood*. 2017;129(20): 2737-2748.

68. Alahmari B, Cooper M, Ziga E, Ritchey J, DiPersio JF, Choi J. Selective targeting of histone modification fails to prevent graft versus host disease after hematopoietic cell transplantation. *PLoS One*. 2018;13(11): e0207609.

69. Souroullas GP, Jeck WR, Parker JS, et al. An oncogenic Ezh2 mutation induces tumors through global redistribution of histone 3 lysine 27 trimethylation. *Nat Med*. 2016; 22(6):632-640.

70. Tan J, Yang X, Zhuang L, et al. Pharmacologic disruption of polycomb-repressive complex 2-mediated gene repression selectively induces apoptosis in cancer cells. *Genes Dev*. 2007;21(9):1050-1063.

71. Du J, Paz K, Flynn R, et al. Pirfenidone ameliorates murine chronic GVHD through inhibition of macrophage infiltration and TGF-β production. *Blood*. 2017;129(18): 2570-2580.

72. Paz K, Flynn R, Du J, et al. Small-molecule BCL6 inhibitor effectively treats mice with nonsclerodermatous chronic graft-versus-host disease. *Blood*. 2019;133(1):94-99.

73. Dubovsky JA, Flynn R, Du J, et al. Ibrutinib treatment ameliorates murine chronic graft-versus-host disease. *J Clin Invest*. 2014; 124(11):4867-4876.

74. Balakrishnan A, Gloude N, Sasik R, Ball ED, Morris GP. Proinflammatory dual receptor T cells in chronic graft-versus-host disease. *Biol Blood Marrow Transplant*. 2017;23(11): 1852-1860.

75. Santos E Sousa P, Ciré S, Conlan T, et al. Peripheral tissues reprogram $CD8^+$ T cells for pathogenicity during graft-versus-host disease. *JCI Insight*. 2018;3(5):97011.

76. Poe JC, Zhang D, Xie J, et al. Single-cell RNA-seq identifies potentially pathogenic B cell populations that uniquely circulate in patients with chronic Gvhd. *Blood*. 2019; 134(suppl 1):874.

77. Zhong H, Liu Y, Xu Z, et al. TGF-β-induced $CD8^+CD103^+$ regulatory T cells show potent therapeutic effect on chronic graft-versus-host disease lupus by suppressing B cells. *Front Immunol*. 2018;9:35.

78. Deng R, Hurtz C, Song Q, et al. Extrafollicular $CD4^+$ T-B interactions are sufficient for inducing autoimmune-like chronic graft-versus-host disease. *Nat Commun*. 2017;8(1):978.

79. Calado DP, Sasaki Y, Godinho SA, et al. The cell-cycle regulator c-Myc is essential for the formation and maintenance of germinal centers. *Nat Immunol*. 2012;13(11):1092-1100.

80. Klein U, Dalla-Favera R. Germinal centres: role in B-cell physiology and malignancy. *Nat Rev Immunol*. 2008;8(1):22-33.